Modeling of bending-torsion couplings in active-bending structures. Application to the design of elastic gridshell.

Thèse n. xxxxx
présenté le 01 décembre 2017
à l'Ecole des Ponts ParisTech
laboratoire Navier
Université Paris-Est

pour l'obtention du grade de Docteur ès Sciences
par

Lionel du Peloux

acceptée sur proposition du jury:

Prof Name Surname, président du jury
Prof Name Surname, directeur de thèse
Prof Name Surname, rapporteur
Prof Name Surname, rapporteur
Prof Name Surname, rapporteur

Paris, Ecole des Ponts ParisTech, 2016

Contents

5 Elastic rod : equilibrium approach

5.1 Introduction

Ici on explique que l'approche par les équations d'équilibre est beaucoup plus directe que l'approche énergétique.

5.1.1 Goals and contribution

Dans ce chapitre, après un bref rappel sur le cadre mathématique d'étude des courbes paramétrique de l'espace, on présente les notions de courbures et de torsion géométrique associées au repère de fraient. On montre ensuite le cas plus général d'un repère mobile quelconque attaché à une courbe gamma. On définit enfin la particularité d'un repère mobile adapté à un courbe, et on présente, en sus du repère de Frenet, une approche différente pour accrocher des repères le long d'une courbe (Bishop / RMF / Zéro-twisting frame)

Ici il faudrait préciser la terminologie des auteurs / équations / hypothèses : Euler-Bernoulli, Navier-Bernoulli, Kirchhoff, Love, Clebesh, Cosserat, Vlassov

5.1.2 Related work

On peu s'instruire dans la publi de Dill [Dil92]. Regarder en particulier le premier chapitre de l'HDR de Neukirch [Neu09]. Regarder également la chronologie des modèles proposée dans la thèse de Theetten [The07]. Pourquoi pas proposer une frise chronologique + un tableau de synthèse des hyptohèses.

[Dil92] **(author?)** [Neu09] [ABW99] [Hoo06] [LL09] [Spi08] [Ant05]

[Neu09] : p69 - [Dil92] : p16

Dans les tentatives dans notre domaine, citer :

Kirchhoff : [Kir50, Kir76]
Clebsch : [Cle83]
Love : [Lov92]
Timoshenko : [Tim21, Tim22, TG51]

"Note that γ having unit speed corresponds to the rod being inextensible; this is not always assumed in the theory, nor is the material frame necessarily assumed to be orthonormal as it is here" [LS96, p. 607]

"Natural frames and the curve angle representation of rod" [LS96, p. 607]

Départ : [Day65] : already includes a rotational DOF !! [Wak80] [Bar99] : revue intéressante de la DR.

3 pts classique : [ABW99] [DBC06]

2 x 3pts : [BAK13]

6 Dofs : [DKZ14]

4Dofs : [dPTL+15] [DZK16]

Dans le champ de l'animation avec élément finis [DLP13] [MPW14]

5.1.3 Overview

Résumé du chapitre

[1] [2] [3]

"The battle between weight and rigidity constitutes, in itself, the single aesthetic theme of art in architecture : and to bring out this conflict in the most varied and clearest way is its office." [Ben91, p. xvii]

> The theory of elastic structures is, by definition, the collection of all reasonable models, proposed during almost three centuries, concerned with simplifying the solutions of problems involving elastic bodies. The equations describing the motion and equilibrium of a three-dimensional elastic body were formulated in full generality during the first half of the nineteenth century, but their solutions are known only in a few cases. [Vil97, p. xvii]

[1] For a shearable rod, the condition that $\boldsymbol{d}_3$ and $\boldsymbol{t}$ coincide is relaxed.

[2] in the directions of the principal axes of inertia of its cross section

[3] The parameter $\bar{s}$, usually chosen as the arc length parameter for the undeformed rod, is no longer the arc length parameter for the deformed rod, since there are deformations of shear and extension. The current arc length of the deformed rod is a function of $\bar{s}$, which is often denoted by $s(\bar{s})$.

> In a deformed state, the center line has no particular reason to remain straight and, in general, $\boldsymbol{d}_1$ and $\boldsymbol{d}_2$ will twist along the center line. However, in the case of small strain that we consider, the triad $(\boldsymbol{d}_1, \boldsymbol{d}_2, \boldsymbol{d}_3)$ remains approximately orthonormal, provided it has been chosen orthonormal in the reference configuration. This is known as the Euler-Bernoulli or Navier-Bernoulli kinematical hypothesis, or sometimes the assumption of unshearable rods. [AAP10, p. 68]

Extension to the case of thin-walled sections by [DA15, Vet14] in the case of ribbons. From the Vlasov

> For thin beams having a slender cross-section, $h \ll w$, the classical rod theory of Kirchhoff is known to be inapplicable. Such beams are usually modeled using Vlasov's theory for thin-walled beams. Vlasov's models can be justified from 3D elasticity but only in the case of moderate deformations, when the cross-sections bend by a small amount. In the present work, however, we have considered large deformations of thin strips. The strip has been modeled as an inextensible plate, and the geometric constraint of inextensibility has been treated exactly : the cross-sections are allowed to bend by a significant amount. Our model extends the classical strip model of Sadowsky, and reformulate it in a way that fits into the classical theory of rods. [DA14, p.]

5.2 Cosserat theory of rods : an introduction

This paragraph gives a (very) brief overview of the *Cosserat theory of rods*, as presented in [Ant05], that accounts for bending, torsion, extension and shear behaviors of slender beams.[4] It gives a larger scope to the basements of the present work – which relies on the *Kirchhoff theory of rods* – as the last is subsumed in this larger theoretical framework. Thus, what is presented in this paragraph could be considered as a reasonable starting point to extend the present work, for instance to take account for shear which might be relevant for some form-finding processes or engineering problems.

This theory was introduce by [Ant74]. It has been largely employed in various fields [SBH95, BAV+10].

Actual configuration

At time t, the *actual* or *deformed* configuration of the rod $\{\boldsymbol{x}, \boldsymbol{d}_1, \boldsymbol{d}_2\}$ is described by its *centerline* $\gamma \in \mathcal{C}^1([0, L] \times \mathbb{R}^3)$, a regular space curve,

$$\begin{array}{rccc} \gamma(t,\cdot): & [0,\overline{L}] & \longrightarrow & \mathbb{R}^3 \\ & \bar{s} & \longmapsto & \boldsymbol{x}(t,\bar{s}) \end{array} \tag{5.1}$$

and two perpendicular[5] unit vector fields :

$$\begin{array}{rccc} (\boldsymbol{d}_1,\boldsymbol{d}_2)(t,\cdot): & [0,\overline{L}] & \longrightarrow & \mathbb{R}^3 \times \mathbb{R}^3 \\ & \bar{s} & \longmapsto & (\boldsymbol{d}_1(t,\bar{s}), \boldsymbol{d}_2(t,\bar{s})) \end{array} \tag{5.2}$$

In addition, we define a third unit vector field as :

$$\boldsymbol{d}_3 = \boldsymbol{d}_1 \times \boldsymbol{d}_2 \tag{5.3}$$

Thus, the centerline is framed with the orthonormal moving frame $\{\boldsymbol{d}_1, \boldsymbol{d}_2, \boldsymbol{d}_3\}$. The unit vectors $\boldsymbol{d}_i(t,\bar{s})$ are called *material directors*.

Note that the centerline is parametrized by $\bar{s}$ which is chosen to be the arc length parameter of the *reference* configuration. It may not coincide with the arc length parameter of the *actual* configuration denoted by $s = s(t,\bar{s})$ as the rod may suffer elongation.

Reference configuration

We now identify a *reference* configuration $\{\overline{\boldsymbol{x}}, \overline{\boldsymbol{d}_1}, \overline{\boldsymbol{d}_2}\}$ of the rod as a stress-free configuration when no external loads are applied to the rod. With no loss of generality, this configuration is assumed to be the configuration at time $t = 0$.

[4] "[we formulate] a general dynamical theory of rods that can undergo large deformations in space by suffering flexure, torsion, extension, and shear. We call the resulting geometrically exact theory the *special Cosserat theory of rods*." [Ant05, p. 270]

[5] For all s : $\boldsymbol{d}_1(s) \perp \boldsymbol{d}_2(s)$.

In this configuration, the rod is assumed to be prismatic. The centerline is chosen to be the curve passing through the cross-section centroids. We call $\bar{s}$ its arc length parameter and $\overline{L}$ its length. The set of rod material points that belong to the plane perpendicular to the centerline at arc length $\bar{s}$ is classically called a *cross-section*. Note that while cross-sections are defined in the *reference* configuration and are planar by definition, there is no reason that this surface stays planar in any other configuration [Dil92, p. 5].

Strains

We decompose the rod deformations in the material frame basis of the *actual* configuration at position $\bar{s}$ of the *reference* configuration $\{\boldsymbol{d}_1, \boldsymbol{d}_2, \boldsymbol{d}_3\}(\bar{s})$.

The deformation of the centerline regarding the variable $\bar{s}$ is described with the help of the strain vector $\boldsymbol{\nu}$ with coordinates $(\nu_1, \nu_2, \nu_3 = 1+\epsilon)^T$ in the material frame basis : [6]

$$\frac{\partial \boldsymbol{x}}{\partial \bar{s}}(t,\bar{s}) = \nu_1(t,\bar{s})\boldsymbol{d}_1(t,\bar{s}) + \nu_2(t,\bar{s})\boldsymbol{d}_2(t,\bar{s}) + \nu_3(t,\bar{s})\boldsymbol{d}_3(t,\bar{s}) \tag{5.4}$$

The deformation of the material frame regarding the variable $\bar{s}$ is described with the help of the strain vector $\boldsymbol{\omega}$ with coordinates $(\kappa_1, \kappa_2, \tau)^T$ in the material frame basis :

$$\frac{\partial \boldsymbol{d}_i}{\partial \bar{s}}(t,\bar{s}) = \boldsymbol{\omega}(t,\bar{s}) \times \boldsymbol{d}_i(t,\bar{s}) \tag{5.5}$$

The velocity of the material frame is described with the help of the spin vector $\boldsymbol{w}$ with coordinates $(w_1, w_2, w_3)^T$ in the material frame basis :

$$\frac{\partial \boldsymbol{d}_i}{\partial t}(t,\bar{s}) = \boldsymbol{w}(t,\bar{s}) \times \boldsymbol{d}_i(t,\bar{s}) \tag{5.6}$$

Now, the spatial derivative regarding $\bar{s}$ will be denoted by a prime $(')$ and the time derivative regardin t by a dot $(\dot{})$.

Parametrization

Because the centerline of the reference configuration is parametrized by arc length, the unit tangent vector is given by :

$$\bar{\boldsymbol{t}}(t,\bar{s}) = \frac{\partial \bar{\boldsymbol{x}}}{\partial \bar{s}}(t,\bar{s}) = \bar{\boldsymbol{x}}'(t,\bar{s}) \quad , \quad \|\bar{\boldsymbol{x}}'\| = 1 \tag{5.7}$$

In the deformed configuration, the centerline is still parametrized by $\bar{s}$ which is no more an arc length parameter as extension happened. Thus, the unit tangent vector is given by :

$$\boldsymbol{t}(t,\bar{s}) = \frac{\boldsymbol{x}'(t,\bar{s})}{\|\boldsymbol{x}'(t,\bar{s})\|} \quad , \quad \|\boldsymbol{x}'\| = \frac{\partial s}{\partial \bar{s}} \neq 1 \tag{5.8}$$

[6] The elongation strain is defined in [Ant05, pp. 283] as : $\nu_3 = \boldsymbol{x}' \cdot (\boldsymbol{d}_1 \times \boldsymbol{d}_2) = \boldsymbol{x}' \cdot \boldsymbol{d}_3 = 1+\epsilon$. ν_1 and ν_2 are called shear strains.

However, this is just a convention and one can switch back to the arc length parametrization in the actual configuration, in which the unit tangent vector is also given by :

$$\boldsymbol{t}(t,s) = \frac{\partial \boldsymbol{x}}{\partial s}(t,s) \quad , \quad \| \frac{\partial \boldsymbol{x}}{\partial s}(t,s) \| = 1 \tag{5.9}$$

Inextensibility

The rod is said to be inextensible if $\epsilon(t,\bar{s}) \ll 1$. In that case, $s(t,\bar{s}) = \bar{s}$ at all time, and the same arc length parametrization is valid for every configurations.

To go further

The reader is invited to refer to [Ant05] to get a deeper understanding of the *Cosserat theory for rods*. The geometric description of a Cosserat rod has been presented in a very generic but still concise manner. This description will be used in the next sections in the narrower scope of the (first order) *Kirchhoff theory for rods* but could be usefully employed for richer theories.

$$\chi \tag{5.10}$$

5.3 Kirchhoff theory of rods

In this section we follow [Dil92] to introduce Kirchhoff theory of rods, where Dill "examine the classical theory of finite displacements of thin rods as developped by Kirchhoff and Clebesch, and presented by Love".

We assume that material and section properties are slowly varying along the centerline. Note that symbols referring to this configuration will carry an overbar.

ces équations sont valables à l'ordre 2 en α [CDL+93] où :

$$\alpha = \max_{s\in[0,L]} \{|\kappa(s)|h, |\bar{\kappa}(s)|h, h/L\} \tag{5.11}$$

Reference (or stress-free) configuration

We consider a *stress-free* configuration of the rod that is called the *reference* configuration.[7] The rod is fully described by its centerline γ and its material frame $\{\boldsymbol{d}_1, \boldsymbol{d}_2, \boldsymbol{d}_3\}$.[8] The set of material points lying in a plane perpendicular to γ defines a *cross section* $(\mathcal{S})$ and is thus a planar surface.

We require that $\gamma \in \mathcal{C}^1$ is at least a regular space curve – that is its tangent vector is continuously defined $\boldsymbol{t} = \frac{d\bar{\boldsymbol{x}}}{ds}$. We denote s its arc length parameter, L its length and $\bar{\boldsymbol{x}}$ the position vector in this configuration :

$$\begin{array}{rccc} \gamma: & [0,L] & \longrightarrow & \mathbb{R}^3 \\ & s & \longmapsto & \bar{\boldsymbol{x}}(s) \end{array} \tag{5.12}$$

We also require that each cross section centroid belong to the centerline. We choose $\boldsymbol{d}_1(s)$ and $\boldsymbol{d}_2(s)$ to be unit vectors aligned with the principal axes of the cross section so they are perpendicular to each other and they lie in the plane of $\mathcal{S}(s)$:

$$\begin{array}{rccc} (\boldsymbol{d}_1, \boldsymbol{d}_2): & [0,L] & \longrightarrow & \mathbb{R}^3 \times \mathbb{R}^3 \\ & s & \longmapsto & (\boldsymbol{d}_1(s), \boldsymbol{d}_2(s)) \end{array} \tag{5.13}$$

For a sufficiently slender rod, the position of material point $\overline{\boldsymbol{\mathcal{P}}}$ in section $\mathcal{S}$ can be expressed through its material coordinates as : [9]

$$\overline{\boldsymbol{\mathcal{P}}}(X_1, X_2, s) = \bar{\boldsymbol{x}}(s) + X_1 \boldsymbol{d}_1(s) + X_2 \boldsymbol{d}_1(s) \tag{5.14}$$

Consequently, in the reference configuration, (X_1, X_2) is a cartesian coordinate system in the plane of the cross section. In this system the local coordinates of the section's centroid

[7] See [AAP10, p. 20] for precisions when such a configuration may not exist.

[8] This description is employed by Antman in his *special Cosserat theory of rods* : "The motion of a special Cosserat rod is defined by three vector-valued functions : $[s_1, s_2] \times \mathbb{R} \ni (s,t) \mapsto \boldsymbol{r}(s,t)$, $\boldsymbol{d}_1(s,t)$, $\boldsymbol{d}_2(s,t) \in \mathbb{E}^3$" [Ant05, p. 270].

[9] The lateral dimension of the rod must be smaller than the radius of curvature. Otherwise, this description would lead to self intersection of cross sections.

are $(0, 0)$.

Finally, we define the third component of the material frame as the unit vector so that $\{\boldsymbol{d}_1, \boldsymbol{d}_2, \boldsymbol{d}_3\}$ form a direct orthonormal basis :

$$\boldsymbol{d}_3 = \boldsymbol{d}_1 \times \boldsymbol{d}_2 = \boldsymbol{t} \tag{5.15}$$

Since the material frame is orthonormal, it's evolution along the *undeformed* centerline is described thanks to the *reference strain vector* $\overline{\boldsymbol{\omega}}$ defined as :

$$\frac{d}{ds}(\boldsymbol{d}_i) = \overline{\boldsymbol{\omega}} \times \boldsymbol{d}_i \tag{5.16}$$

In the reference configuration, because the centerline is parametrized by arc length, the strain vector components expressed in the material frame basis are given by :

$$\overline{\boldsymbol{\kappa b}} = \boldsymbol{t} \times \boldsymbol{t}' \tag{5.17a}$$

$$\overline{\omega}_1 = \overline{\kappa_1} = \boldsymbol{\kappa b} \cdot \boldsymbol{d}_1 \tag{5.17b}$$

$$\overline{\omega}_2 = \overline{\kappa_2} = \boldsymbol{\kappa b} \cdot \boldsymbol{d}_2 \tag{5.17c}$$

$$\overline{\omega}_3 = \overline{\tau} = \boldsymbol{d}_1' \cdot \boldsymbol{d}_2 = -\boldsymbol{d}_2' \cdot \boldsymbol{d}_1 \tag{5.17d}$$

Actual (or deformed) configuration

We now examine the motion of the rod and we call *actual* configuration or *deformed* configuration its configuration at time t. In this configuration the rod undergoes internal stresses under body loads, external loads and constrains. A material point $\overline{\boldsymbol{\mathcal{P}}}$ is transported to $\boldsymbol{\mathcal{P}}$. The actual rod is fully described by its centerline $\gamma_t = \gamma(t)$, its material frame $\{\boldsymbol{d}_1, \boldsymbol{d}_2, \boldsymbol{d}_3\}(t)$ and a local displacement field $\boldsymbol{u}(t)$. The components $(u_1, u_2, u_3)^T$ of the local displacement field expressed in the material frame basis are assumed to be small in Kirchhoff's theory.[10]

In his theory, Kirchhoff shows that the material frame in the reference configuration deforms in a rigid-body manner so that it remains orthonormal.[11] Remark that this is different than assuming that cross sections deform in a rigid-body manner, which is known as the *Euler-Bernoulli* hypothesis and is equivalent to the special case $\boldsymbol{u} = \boldsymbol{0}$. More over, the theory assumes that the material frame remains adapted to the centerline during deformation so that transverse shear deformations are neglected.[12]

[10] Note that this hypothesis is the one made by Kirchhoff and does not correspond to the well-known *Euler-Bernoulli* or *Navier-Bernoulli* assumption where the sections remain planar, undeformed and normal to the centerline during the rod deformation. In particular, torsion is responsible for the warping of cross sections – that is sections don't remain planar – and leads to a distinct value of the twist modulus (J). This is clearly stipulated in [Dil92, AAP10] but is often treated with confusion in the literature.

[11] This is true within an error $O(\alpha^2)$ as explained in [CDL+93].

[12] This is also known as the "unsherable" assumption. Indeed, if $\frac{\partial \boldsymbol{x}}{\partial s} = \nu_k \boldsymbol{d}_k = (1+\epsilon)\boldsymbol{d}_3 \Leftrightarrow \nu_1 = \nu_2 = 0$.

The centerline of the rod is deformed into a new space curve with position vector $\boldsymbol{x}$:

$$\begin{aligned} \gamma_t : \quad [0, L] &\longrightarrow \mathbb{R}^3 \\ s &\longmapsto \boldsymbol{x}(s) \end{aligned} \tag{5.18}$$

The curve is still parametrized by the arc length parameter (s) of the *reference* configuration as the constitutive laws will be expressed relatively to this configuration. But note that s is no more the arc length parameter of the *deformed* centerline as the rod may have suffer axial extension.[13] The extension of the centerline is characterized by ϵ defined such that :

$$\frac{\partial \boldsymbol{x}}{\partial s} = \nu_3 \boldsymbol{d}_3 = (1+\epsilon)\boldsymbol{d}_3 \tag{5.19}$$

However, one can parametrized the deformed centerline by its own arc length parameter, denoted s_t. We call L_t the length of the deformed centerline and g_t the $\mathcal{C}^1$ diffeomorphisme that maps s onto s_t ($s_t = g_t(s) \Leftrightarrow s = g_t^{-1}(s_t)$). Thus, the centerline is also described as :

$$\begin{aligned} \gamma_t : \quad [0, L_t] &\longrightarrow \mathbb{R}^3 \\ s_t &\longmapsto \boldsymbol{x}(s_t) \end{aligned} \tag{5.20}$$

Because s_t is the arc length parameter of γ_t the following relations hold :

$$\frac{\partial \boldsymbol{x}}{\partial s_t} = \boldsymbol{t} = \boldsymbol{d}_3 \tag{5.21a}$$

$$\frac{\partial s_t}{\partial s} = \nu_3 = 1 + \epsilon \tag{5.21b}$$

Since the material frame is orthonormal, it's evolution along the *deformed* centerline is described thanks to the *actual strain vector* $\boldsymbol{\omega}$ defined as :

$$\frac{\partial}{\partial s}(\boldsymbol{d}_i) = \boldsymbol{\omega} \times \boldsymbol{d}_i \tag{5.22}$$

Note that the strain vector is defined relatively to the arc length (s) of the *reference* configuration and not the arc length of the *actual* configuration (s_t). Thus the strain vector components expressed in the material frame basis are given by :

$$\boldsymbol{\kappa b} = \boldsymbol{t} \times \frac{\partial \boldsymbol{t}}{\partial s_t} = (1+\epsilon)\boldsymbol{t} \times \boldsymbol{t}' \tag{5.23a}$$

$$\omega_1 = (1+\epsilon)\kappa_1 = (1+\epsilon)\boldsymbol{\kappa b} \cdot \boldsymbol{d}_1 \tag{5.23b}$$

$$\omega_2 = (1+\epsilon)\kappa_2 = (1+\epsilon)\boldsymbol{\kappa b} \cdot \boldsymbol{d}_2 \tag{5.23c}$$

$$\omega_3 = (1+\epsilon)\tau = (1+\epsilon)\boldsymbol{d}_1' \cdot \boldsymbol{d}_2 = -(1+\epsilon)\boldsymbol{d}_2' \cdot \boldsymbol{d}_1 \tag{5.23d}$$

It is important that the material strains (ω_1, ω_2, ω_3) are corrected according to the extension of the rod. These are the strains employed in the classical constitutive laws that lead to the determination of the internal axial force and moments. In the case of an inextensible rod ($\epsilon = 0$) there is no need to make the distinction between s_t and s. The

[13] In Kirchhoff's theory, rods are not supposed to be strictly inextensible but extension has to remain small.

same parameter is an arc length parameter for all configurations at all time.

Balance of momentum

Local displacements

Local strains

Dynamical equations

5.4 Dynamical equations for Kirchhoff rods

référence importante pour la rod [MLG13] , [Vil97, p. 109]. modeling of DNA molecules, pipes or hosing, plant, hair, surgery,

Pour la rod extensible : [CH02]

Unshearable. The rod can be considered as unshearable if $\nu_1 \ll 1$ and $\nu_2 \ll 1$. In that case, the third material vector remains parallel to the centerline $\boldsymbol{d}_3 \times \boldsymbol{t} = 0$ and the material frame is adapted to the centerline. However, in the case of small strain that we consider, the triad $(\boldsymbol{d}_1, \boldsymbol{d}_2, \boldsymbol{d}_3)$ remains approximately orthonormal, provided it has been chosen orthonormal in the reference configuration. This is known as the Euler-Bernoulli or Navier-Bernoulli kinematical hypothesis, or sometimes the assumption of unshearable rods.

Attention, en faisant l'hypothèse du repère mobile attaché à la courbe pour représenter les sections, ont fait une hypothèse sérieuse.

A thorough order-of-magnitude analysis is exposed in [Dil92, CDL+93]

A larger scope full development is given in chapter 8 from [Ant05, pp. 270-274]

[14] [15]

“The classical elastic rod theory of Kirchhoff (1859), called the kinetic analogue, is is a special case of our rod theory [...]” [Ant05, p. 238]

“If the reference configuration is not straight, then the uncoupling between the extension and the flexure and shear is lost.” [Ant05, p. 341]

5.4.1 Assumptions

in which the rod is considered under the following assumptions : [16]

1. The centerline of the rod is inextensible
2. Cross-sections remain plane, undistorted, and normal to the axis of the rod[17]
3. Internal moments depend linearly upon the curvature of the centerline and the twist of sections.

[14] “We discuss here the dynamical equations of a theory of elastic rods that is due to Kirchhoff and Clebsch. This properly invariant theory is applicable to motions in which the strains relative to an undistorted configuration remain small, although rotations may be large. It is constructed to be a first-order theory, i.e., a theory that is complete to within an error of order two in an appropriate dimensionless measure of thickness, curvature, twist, and extension.” [CDL+93, p. 1]

[15] “In a first-order theory of thin rods, one can treat the rod as inextensible [. . .]” [CDL+93, p. 1]

[16] This assumptions are also known as the *Kirchhoff-Love* assumptions.

[17] This assumption is also known as the *Euler-Bernoulli* kinematical hypothesis.

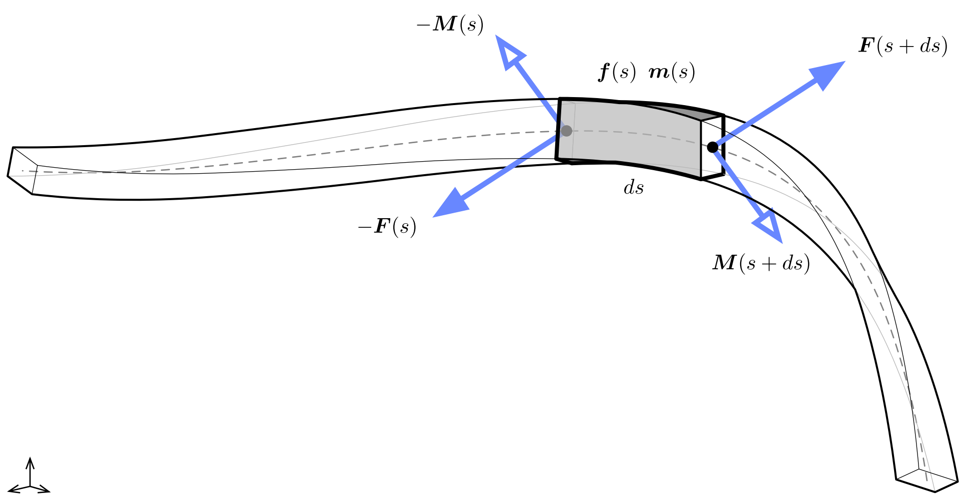

Figure 5.1 – Internal forces ($\boldsymbol{F}$) and moments ($\boldsymbol{M}$) acting on an infinitesimal beam slice of length ds. The beam is also subject to distributed external forces ($\boldsymbol{f}$) and moments ($\boldsymbol{m}$). By convention, internal forces and moments are forces and moments applied by the right part to the left part of the beam.

ces équations sont valables à l'ordre 2 en α où :

$$\alpha = \max_{s\in[0,L]} \{|\kappa(s)|h, |\bar{\kappa}(s)|h, h/L\} \tag{5.24}$$

On fait par ailleurs l'hypothèse inextensible pour la dérivation du repère materiel.

dynamical equations

Writing the balance of linear and angular momentum of a beam slice of infinitesimal yields to the dynamic Kirchhoff equations for a slender beam. An extensive proof of this development is available in [Dil92].

18 19 20

[18]"The principal normal, binormal, and torsion of the axis, viewed as an element of a space curve, have no special significance in the theory of rods. Use of those special directions as base vectors does not simplify the theory and can mislead the reader into attributing significance to them when none exists. In particular, the curvature of the rod should not be confused with the curvature of the space curve which the axis forms." [Dil92, p. 5]

[19]"Kirchhoff's theory can only apply to that class of problems for three dimensional bodies such that the loads on the sides are relatively small and slowly varying. The dominate mode of deformation must be a global bending and twisting with small axial extension. If there are substantial local variations in curvatures or substantial transverse shears, his theory of bending of rods will not provide a satisfactory first approximation." [Dil92, p. 18]

[20]"There are no constitutive relations for F_1 or F_2. They are determined by the balance of momentum as in the elementary linear theory of bending of rods." [Dil92, p. 15]

5.4.2 Balance of linear momentum

On fait un bilan sur une tranche d'épaisseur ds, de centre de gravité G positionné en $\boldsymbol{x}_G$:

$$\boldsymbol{F}(s+ds) - \boldsymbol{F}(s) + \boldsymbol{f}(s)ds = \left(\frac{\partial \boldsymbol{F}}{\partial s}(s) + \boldsymbol{f}(s)\right) ds = (\rho S ds)\ddot{\boldsymbol{x}}_G \tag{5.25}$$

Which leads to the first equation of Kirchhoff law :

$$\frac{\partial \boldsymbol{F}}{\partial s} + \boldsymbol{f} = \rho S \ddot{\boldsymbol{x}}_G \tag{5.26}$$

5.4.3 Balance of angular momentum

On fait un bilan sur une tranche d'épaisseur ds, de centre de gravité G positionné en $\boldsymbol{x}_G$. On applique le théorème du moment cinétique dans un référentiel inertiel :

$$\begin{aligned}\frac{d}{dt}(dI_G) &= \boldsymbol{M}(s+ds) - \boldsymbol{M}(s) + \boldsymbol{m}(s)ds + (\tfrac{1}{2}ds\boldsymbol{x}') \times \boldsymbol{F}(s+ds) + (-\tfrac{1}{2}ds\boldsymbol{x}') \times -\boldsymbol{F}(s) \\ &= \left(\frac{\partial \boldsymbol{M}}{\partial s}(s) + \boldsymbol{m}(s) + \boldsymbol{x}' \times \boldsymbol{F}(s)\right) ds\end{aligned} \tag{5.27}$$

L'évolution temporelle des vecteurs matériels est cette fois décrite par un vecteur de Darboux temporel – spin vector in [CDL+93] – noté $\boldsymbol{\Lambda}$ tel que : Compatibility equation between the curvature vector and the spin vector ($\kappa\dot{\boldsymbol{b}} - \boldsymbol{\Lambda}' = \boldsymbol{\Lambda} \times \kappa\boldsymbol{b}$).

$$\dot{\boldsymbol{d}}_i(s) = \boldsymbol{\Lambda}(t) \times \boldsymbol{d}_i(s) \quad , \quad \boldsymbol{\Lambda}(t) = \begin{bmatrix}\Lambda_3(t)\\ \Lambda_1(t)\\ \Lambda_2(t)\end{bmatrix} \tag{5.28}$$

Les lois de composition / dérivation de la mécanique nous permettent décrire :

$$\frac{d}{dt}(dI_G) = dI_G\dot{\boldsymbol{\Lambda}} + \boldsymbol{\Lambda} \times dI_G \tag{5.29}$$

Qu'est ce qu'on met dans dI_G ? Et bien tout simplement l'opérateur d'inertie de la section, qui s'exprime à l'aide des moments quadratiques des directions principales de la façon suivante, dans la base des directions principales d'inertie au premier ordre en ds :

$$dI_G = \begin{bmatrix} dI_{G3} & 0 & 0\\ 0 & dI_{G1} & 0\\ 0 & 0 & dI_{G2}\end{bmatrix} \simeq \rho ds \begin{bmatrix} I_1 + I_2 & 0 & 0\\ 0 & I_1 & 0\\ 0 & 0 & I_2\end{bmatrix} \tag{5.30}$$

Where :

$$dI_{G3} = \int_V \rho(x_1^2 + x_2^2)\, dV \simeq \rho ds \int_V (x_1^2 + x_2^2)\, dx_1 dx_2 \simeq \rho ds (I_1 + I_2) \tag{5.31a}$$

$$dI_{G1} = \int_V \rho(x_2^2 + x_3^2)\, dV \simeq \rho ds \int_V x_2^2\, dx_1 dx_2 \simeq \rho ds I_1 \tag{5.31b}$$

$$dI_{G2} = \int_V \rho(x_1^2 + x_3^2)\, dV \simeq \rho ds \int_V x_1^2\, dx_1 dx_2 \simeq \rho ds I_2 \tag{5.31c}$$

Et l'on peut alors écrire la seconde loi de Kirchhoff sous la forme suivante :

$$\frac{\partial \boldsymbol{M}}{\partial s}(s) + \boldsymbol{m}(s) + \boldsymbol{x}' \times \boldsymbol{F}(s) = \rho \begin{bmatrix} (I_1 + I_2)\dot{\Lambda}_3 + (I_2 - I_1)\Lambda_1\Lambda_2 \\ I_1(\dot{\Lambda}_1 + \Lambda_2\Lambda_3) \\ I_2(\dot{\Lambda}_2 - \Lambda_3\Lambda_1) \end{bmatrix} \tag{5.32}$$

On peut alors conclure sur l'expression de l'equation de kirchoff : [21,22]

$$\frac{\partial \boldsymbol{M}}{\partial s}(s) + \boldsymbol{m}(s) + \boldsymbol{d}_3 \times \boldsymbol{F}(s) = I_1 \boldsymbol{d}_1 \times \ddot{\boldsymbol{d}}_1 + I_2 \boldsymbol{d}_2 \times \ddot{\boldsymbol{d}}_2 \tag{5.33}$$

5.5 Equations of motion

5.5.1 Constitutive equations

"An order-of-magnitude analysis leading ..."

Attention, pas d'effort normal par loi constitutive en principe car on est dans un modèle inextensible. L'effort normal est calculé par la loi d'équilibre avec les moments et/ou efforts tranchants. Ici, on postulera tout de même une telle loi constitutive pour la résolution numérique. Ce qui nous amène à considérer une tige quasiment inextensible.

point à creuser. en gros je suis entrain de dire que dans le modèle classique à 3DOF type Douthe ou Barnes, il n'est pas nécessaire d'introduire la raideur axiale (mais alors où intervient la section ?). L'effort normal est déduit des équations d'équilibre.

En fait cela ne semble pas possible. Il faut alors revenir à l'équation constitutive qui donne l'effort normal, mais alors quid de l'hypothèse quasistatique ?

Dans le fond, l'hyptohèse d'inextensibilité c'est dire que les déformations axiales sont négligeable devant les autres modes de déformation (flexion et/ou torsion). Mais pour caractériser l'effort normal lui même, il faut bien considérer une élongation.

Ou alors, peut-être qu'il faut comprendre que l'effort normal est déduit uniquement des conditions aux limites et/ou éventuellement des efforts extérieurs appliqués à la centerline.

Pour comprendre le traitement de l'inextensibilité, regarder [Ant05] p50. Qu'apporte l'hypothèse d'inextensibilité. Est-elle raisonnable. Tps de calcul par rapport au cas

[21] Recall that : $\dot{\boldsymbol{d}}_i = \boldsymbol{\Lambda} \times \boldsymbol{d}_i$

[22] Remark that : $(\boldsymbol{\Lambda} \times \dot{\boldsymbol{d}}_i) \times \boldsymbol{d}_i = \Lambda_i(\boldsymbol{\Lambda} \times \dot{\boldsymbol{d}}_i)$

extensible.

$$\boldsymbol{N} = ES\epsilon\boldsymbol{d}_3 \tag{5.34a}$$
$$\boldsymbol{M_1} = EI_1(\kappa_1 - \overline{\kappa_1})\boldsymbol{d}_1 \tag{5.34b}$$
$$\boldsymbol{M_2} = EI_2(\kappa_2 - \overline{\kappa_2})\boldsymbol{d}_2 \tag{5.34c}$$
$$\boldsymbol{Q} = [GJ(\theta' - \bar{\theta}') - EC_w(\theta''' - \bar{\theta}''')]\boldsymbol{d}_3 \tag{5.34d}$$

where :

$$I_1 = \int_S x_2^2 \, dx_1 dx_2 \tag{5.35}$$

$$I_2 = \int_S x_1^2 \, dx_1 dx_2 \tag{5.36}$$

$$J = \int_S (x_1^2 + x_2^2 + x_1 \frac{\partial \phi}{\partial x_2} - x_2 \frac{\partial \phi}{\partial x_1}) \, dx_1 dx_2 \tag{5.37}$$

with $\phi(x_1, x_2)$ is the warping function of the cross section.

5.5.2 Internal forces and moments

Efforts internes de coupure :

$$\boldsymbol{F}_{int} = N\boldsymbol{d}_3 + F_1\boldsymbol{d}_1 + F_2\boldsymbol{d}_2 \tag{5.38a}$$
$$\boldsymbol{M}_{int} = Q\boldsymbol{d}_3 + M_1\boldsymbol{d}_1 + M_2\boldsymbol{d}_2 \tag{5.38b}$$

Efforts externes appliqués linéiques :

$$\boldsymbol{f}_{ext} = f_3\boldsymbol{d}_3 + f_1\boldsymbol{d}_1 + f_2\boldsymbol{d}_2 \tag{5.39a}$$
$$\boldsymbol{m}_{ext} = m_3\boldsymbol{d}_3 + m_1\boldsymbol{d}_1 + m_2\boldsymbol{d}_2 \tag{5.39b}$$

5.5.3 Rod dynamic

First Kirchhoff law projecting on the material frame basis :

$$N' + \kappa_1 F_2 - \kappa_2 F_1 + f_3 = \rho S \ddot{x}_3 \tag{5.40a}$$
$$F_1' + \kappa_2 N - \tau F_2 + f_1 = \rho S \ddot{x}_1 \tag{5.40b}$$
$$F_2' - \kappa_1 N + \tau F_1 + f_2 = \rho S \ddot{x}_2 \tag{5.40c}$$

Qu'on écrit vectoriellement :

$$\boldsymbol{F}' + \boldsymbol{\Omega} \times \boldsymbol{F} + \boldsymbol{f}_{ext} = \rho S \ddot{\boldsymbol{x}} \quad with \quad \boldsymbol{F}' = \begin{bmatrix} F_1' & F_2' & N' \end{bmatrix}^T \tag{5.41}$$

This is nothing but the application of the transport theorem when differentiating a vector expressed in the material frame :

$$\left.\frac{\partial \boldsymbol{F}}{\partial s}\right|_{global} = \left.\frac{\partial \boldsymbol{F}}{\partial s}\right|_{local} + \boldsymbol{\Omega}(s) \times \boldsymbol{F} \tag{5.42}$$

Second Kirchhoff law projecting on the material frame basis : [23]

$$Q' + \kappa_1 M_2 - \kappa_2 M_1 + m_3 = (I_1 + I_2)\dot{\Lambda}_3 + (I_2 - I_1)\Lambda_1\Lambda_2 \tag{5.43a}$$
$$M_1' + \kappa_2 Q - \tau M_2 - F_2 + m_1 = I_1(\dot{\Lambda}_1 + \Lambda_2\Lambda_3) \tag{5.43b}$$
$$M_2' - \kappa_1 Q + \tau M_1 + F_1 + m_2 = I_2(\dot{\Lambda}_2 - \Lambda_3\Lambda_1) \tag{5.43c}$$

Qu'on écrit vectoriellement :

$$\boldsymbol{M}' + \boldsymbol{\Omega} \times \boldsymbol{M} + \boldsymbol{m}_{ext} + \boldsymbol{d}_3 \times \boldsymbol{F} = I_1 \boldsymbol{d}_1 \times \ddot{\boldsymbol{d}}_1 + I_2 \boldsymbol{d}_2 \times \ddot{\boldsymbol{d}}_2 \tag{5.44}$$
$$with \quad \boldsymbol{M}' = \begin{bmatrix} M_1' & M_2' & Q' \end{bmatrix}^T \tag{5.45}$$

This is nothing but the application of the transport theorem when differentiating a vector expressed in the material frame :

$$\left.\frac{\partial \boldsymbol{M}}{\partial s}\right|_{global} = \left.\frac{\partial \boldsymbol{M}}{\partial s}\right|_{local} + \boldsymbol{\Omega}(s) \times \boldsymbol{M} \tag{5.46}$$

[23] As explained in [Dil92, p. 18], if the inextensibility assumption does not hold, the right terms to consider are $-(1+\epsilon)F_2$ in eq. (5.43b) and $(1+\epsilon)F_1$ in eq. (5.43c).

5.6 Geometric interpretation

The previous section has established the dynamical equations for elastic rods. This section gives a simple and straight forward geometric interpretation of this equations as they can be

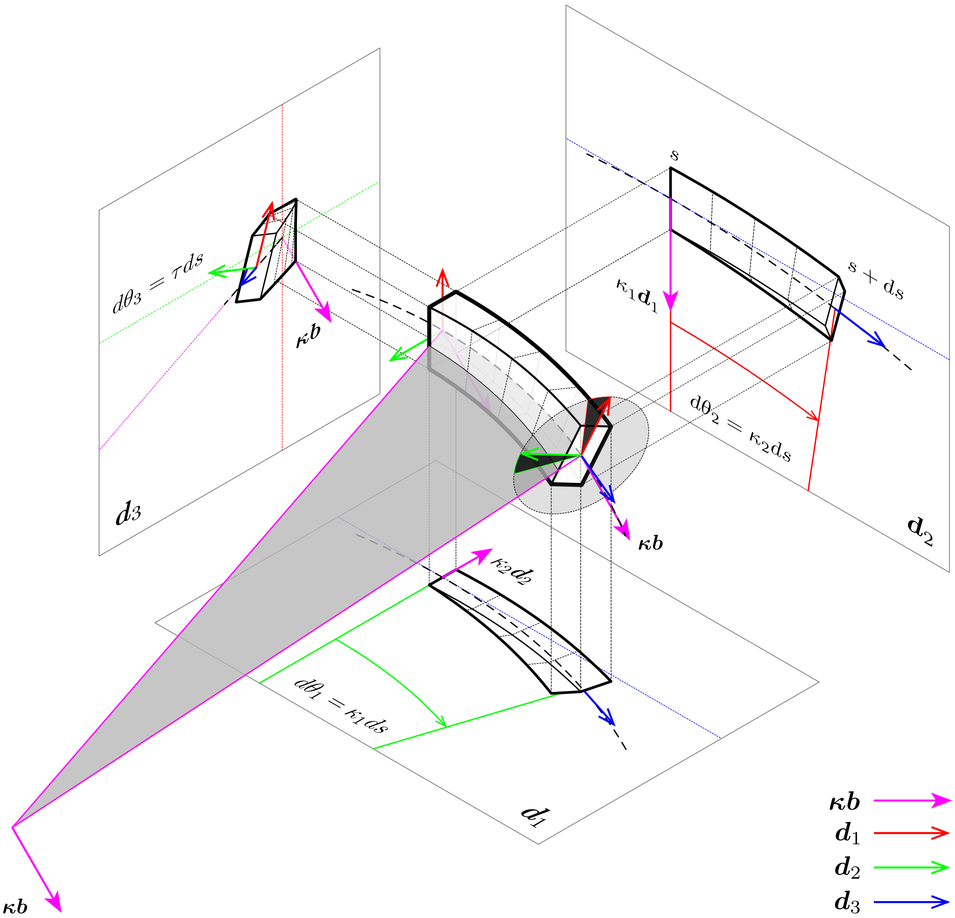

Figure 5.2 – Osculating circles for a spiral curve at different parameters.

5.7 Numerical resolution

5.7.1 Main hypothesis

On néglige les forces d'inertie liées à la rotation de l'élément (devant quoi ?? traitement quasi-statique par rapport à la rotation). Cette hypothèse est faite explicitement chez Florence Bertail :

"neglecting inertial momentum due to the vanishing cross-section lead to the following dynamic equations for a Kirchhoff rod" [CBd13]

> It follows that ω_1 and ω_2 can be neglected in the kinetic energy [...]. However, ω_3, which provides the angular momentum about the axis of the rod, must be retained, This assumption of Kirchhoff is consistent with the technical theory of beams where rotary inertia is known to provide corrections to the natural frequencies of vibration of $O(\alpha^2)$ if the length measure is the half-wave length. [Dil92, p. 17]

Cette hypothèse est faite mais passée sous silence chez Douthe, Adriaenssen, D'Amico lorsqu'ils déduisent l'effort tranchant du moment de flexion.

Principe :

- les équations constitutives permettent le calcul de M_1, M_2, Q à partir de la géométrie $\{\boldsymbol{x}, \theta\}$.

- La seconde loi de kirchhoff projetée sur les axes matériels 1 et 2 de la section me donnent accès aux efforts tranchants T_1 et T_2.

- La seconde loi de kirchhoff projetée sur les axes matériel 3 (tangente à la centerline) de la section me donnent l"hypothèse quasi-statique de Audoly.

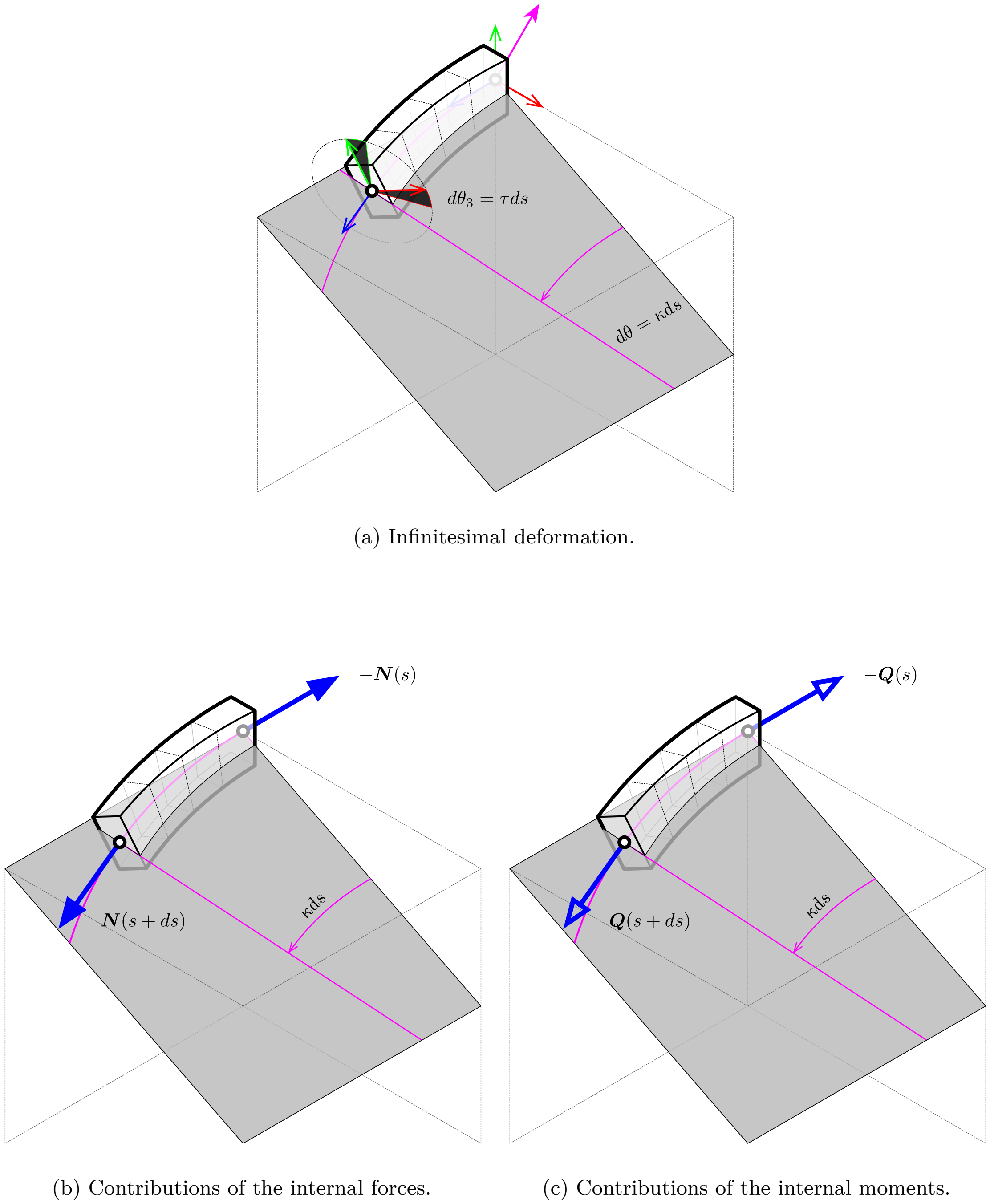

Figure 5.3 – Influence of the curvature (κ) in the deflection of internal forces and moments along the centerline.

Contributions to the balance of forces

$\boldsymbol{N}(s+ds)$ is deflected from $\boldsymbol{d}_3(s)$ by the rotation of angle κds around $\boldsymbol{\kappa b}$ (fig. 5.3b). Thus, its contribution to the balance of forces onto $\boldsymbol{d}_3(s)$ is :

$$N(s+ds)\cos(\kappa ds) - N(s) = N'(s)ds + o(ds)$$

Contributions to the balance of moments

$\boldsymbol{Q}(s+ds)$ is deflected from $\boldsymbol{d}_3(s)$ by the rotation of angle κds around $\boldsymbol{\kappa b}$ (fig. 5.3c). Thus, its contribution to the balance of moments onto $\boldsymbol{d}_3(s)$ is :

$$Q(s+ds)\cos(\kappa ds) - Q(s) = Q'(s)ds + o(ds)$$

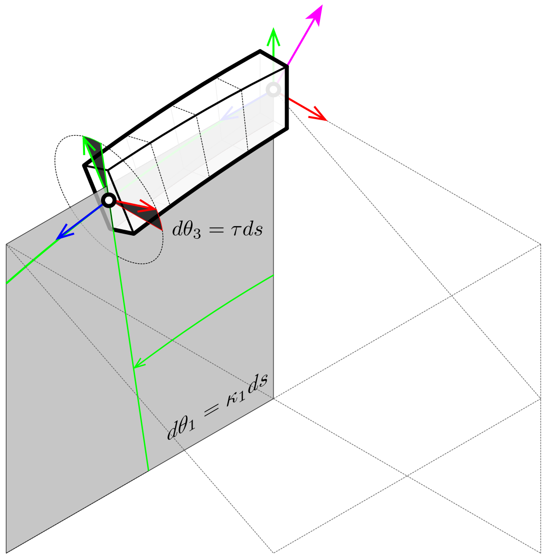

(a) Infinitesimal deformation.

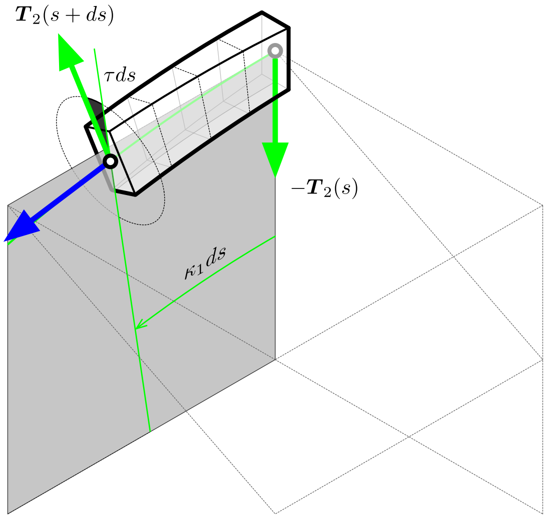

(b) Contributions of the internal forces.

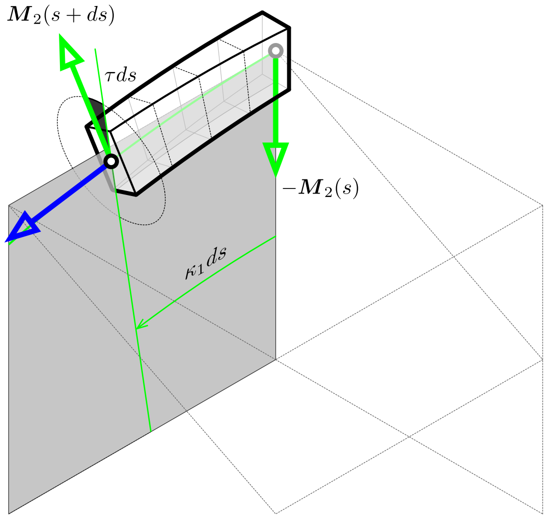

(c) Contributions of the internal moments.

Figure 5.4 – Influence of the first material curvature (κ_1) in the deflection of internal forces and moments along the centerline.

Contributions to the balance of forces

$\boldsymbol{T}_2(s+ds)$ is deflected from $\boldsymbol{d}_2(s)$ by the combined rotations of angle τds around $\boldsymbol{d}_3$ and $\kappa_2 ds$ around $\boldsymbol{d}_2$ (fig. 5.4b). Thus, its contribution to the balance of forces onto $\boldsymbol{d}_1(s)$ is :

$$-T_2(s+ds)\sin(\tau ds)\cos(\kappa_2 ds) = -\tau T_2(s)ds + o(ds)$$

$\boldsymbol{T}_2(s+ds)$ is deflected from $\boldsymbol{d}_2(s)$ by the combined rotations of angle τds around $\boldsymbol{d}_3$ and $\kappa_1 ds$ around $\boldsymbol{d}_1$ (fig. 5.4b). Thus, its contribution to the balance of forces onto $\boldsymbol{d}_2(s)$ is :

$$-T_2(s) + T_2(s+ds)\cos(\tau ds)\cos(\kappa_1 ds) = T_2'(s)ds + o(ds)$$

$\boldsymbol{T}_2(s+ds)$ is deflected from $\boldsymbol{d}_2(s)$ by the combined rotations of angle τds around $\boldsymbol{d}_3$ and $\kappa_1 ds$ around $\boldsymbol{d}_1$ (fig. 5.4b). Thus, its contribution to the balance of forces onto $\boldsymbol{d}_3(s)$ is :

$$T_2(s+ds)\cos(\tau ds)\sin(\kappa_1 ds) = \kappa_1 T_2(s)ds + o(ds)$$

$\boldsymbol{N}(s+ds)$ is deflected from $\boldsymbol{d}_3(s)$ by the combined rotations of angle $\kappa_2 ds$ around $\boldsymbol{d}_2$ and $\kappa_1 ds$ around $\boldsymbol{d}_1$ (fig. 5.4b). Thus, its contribution to the balance of forces onto $\boldsymbol{d}_2(s)$ is :

$$-N(s+ds)\cos(\kappa_2 ds)\sin(\kappa_1 ds) = -\kappa_1 N(s)ds + o(ds)$$

Contributions to the balance of moments

$\boldsymbol{T}_2(s+ds)$ is deflected from the plane normal to $\boldsymbol{d}_1(s)$ by a rotation of angle τds around $\boldsymbol{d}_3$ (fig. 5.4b). It produces a moment around $\boldsymbol{d}_1$ with the lever arm $b = \cos(\kappa_2 ds)ds$. Thus, its contribution to the balance of moments onto $\boldsymbol{d}_1(s)$ is :

$$-T_2(s+ds)\cos(\tau ds)(\cos(\kappa_2 ds)ds) = -T_2(s)ds + o(ds)$$

$\boldsymbol{M}_2(s+ds)$ is deflected from $\boldsymbol{d}_2(s)$ by the combined rotations of angle τds around $\boldsymbol{d}_3$ and $\kappa_2 ds$ around $\boldsymbol{d}_2$ (fig. 5.4c). Thus, its contribution to the balance of moments onto $\boldsymbol{d}_1(s)$ is :

$$-M_2(s+ds)\sin(\tau ds)\cos(\kappa_2 ds) = -\tau M_2(s)ds + o(ds)$$

$\boldsymbol{M}_2(s+ds)$ is deflected from $\boldsymbol{d}_2(s)$ by the combined rotations of angle τds around $\boldsymbol{d}_3$ and $\kappa_1 ds$ around $\boldsymbol{d}_1$ (fig. 5.4c). Thus, its contribution to the balance of moments onto $\boldsymbol{d}_2(s)$ is :

$$-M_2(s) + M_2(s+ds)\cos(\tau ds)\cos(\kappa_1 ds) = M_2'(s)ds + o(ds)$$

$\boldsymbol{M}_2(s+ds)$ is deflected from $\boldsymbol{d}_2(s)$ by the combined rotations of angle τds around $\boldsymbol{d}_3$ and $\kappa_1 ds$ around $\boldsymbol{d}_1$ (fig. 5.4c). Thus, its contribution to the balance of moments onto $\boldsymbol{d}_3(s)$ is :

$$M_2(s+ds)\cos(\tau ds)\sin(\kappa_1 ds) = \kappa_1 M_2(s)ds + o(ds)$$

$\boldsymbol{Q}(s+ds)$ is deflected from $\boldsymbol{d}_3(s)$ by the combined rotations of angle $\kappa_2 ds$ around $\boldsymbol{d}_2$ and $\kappa_1 ds$ around $\boldsymbol{d}_1$ (fig. 5.4c). Thus, its contribution to the balance of moments onto $\boldsymbol{d}_2(s)$ is :

$$-Q(s+ds)\cos(\kappa_2 ds)\sin(\kappa_1 ds) = -\kappa_1 Q(s)ds + o(ds)$$

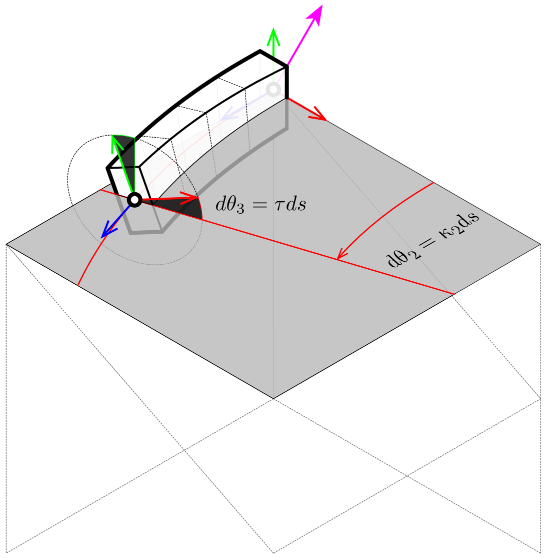

(a) Infinitesimal deformation.

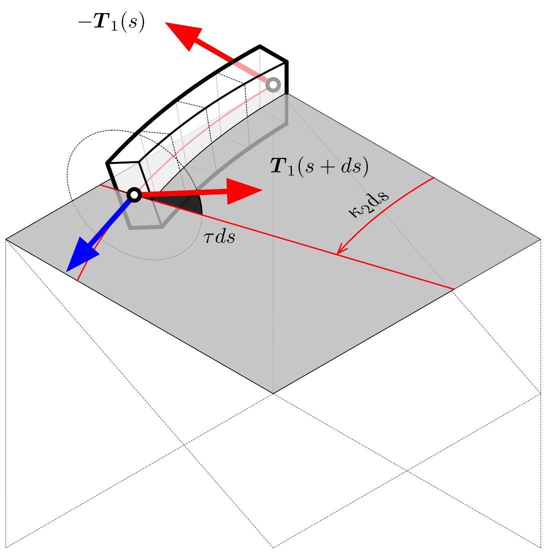

(b) Contributions of the internal forces.

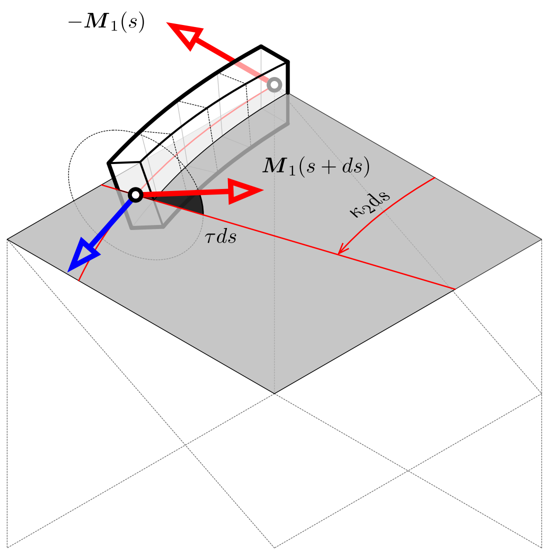

(c) Contributions of the internal moments.

Figure 5.5 – Influence of the second material curvature (κ_2) in the deflection of internal forces and moments along the centerline.

Contributions to the balance of forces

$\boldsymbol{T}_1(s+ds)$ is deflected from $\boldsymbol{d}_1(s)$ by the combined rotations of angle τds around $\boldsymbol{d}_3$ and $\kappa_2 ds$ around $\boldsymbol{d}_2$ (fig. 5.5b). Thus, its contribution to the balance of forces onto $\boldsymbol{d}_1(s)$ is :

$$-T_1(s) + T_1(s+ds)\cos(\tau ds)\cos(\kappa_2 ds) = T_1'(s)ds + o(ds)$$

$\boldsymbol{T}_1(s+ds)$ is deflected from $\boldsymbol{d}_1(s)$ by the combined rotations of angle τds around $\boldsymbol{d}_3$ and $\kappa_1 ds$ around $\boldsymbol{d}_1$ (fig. 5.5b). Thus, its contribution to the balance of forces onto $\boldsymbol{d}_2(s)$ is :

$$T_1(s+ds)\sin(\tau ds)\cos(\kappa_1 ds) = \tau T_1(s)ds + o(ds)$$

$\boldsymbol{T}_1(s+ds)$ is deflected from $\boldsymbol{d}_1(s)$ by the combined rotations of angle τds around $\boldsymbol{d}_3$ and $\kappa_2 ds$ around $\boldsymbol{d}_2$ (fig. 5.5b). Thus, its contribution to the balance of forces onto $\boldsymbol{d}_3(s)$ is :

$$-T_1(s+ds)\cos(\tau ds)\sin(\kappa_2 ds) = -\kappa_2 T_1(s)ds + o(ds)$$

$\boldsymbol{N}(s+ds)$ is deflected from $\boldsymbol{d}_3(s)$ by the combined rotations of angle $\kappa_1 ds$ around $\boldsymbol{d}_1$ and $\kappa_2 ds$ around $\boldsymbol{d}_2$ (fig. 5.5b). Thus, its contribution to the balance of forces onto $\boldsymbol{d}_1(s)$ is :

$$N(s+ds)\cos(\kappa_1 ds)\sin(\kappa_2 ds) = \kappa_2 N(s)ds + o(ds)$$

Contributions to the balance of moments

$\boldsymbol{T}_1(s+ds)$ is deflected from the plane normal to $\boldsymbol{d}_2(s)$ by the angle τds around $\boldsymbol{d}_3$ along ds (fig. 5.5b). It produces a moment around $\boldsymbol{d}_2$ with the lever arm $b = \cos(\kappa_1 ds)ds$. Thus, its contribution to the balance of moments onto $\boldsymbol{d}_2(s)$ is :

$$T_1(s+ds)\cos(\tau ds)(\cos(\kappa_1 ds)ds) = T_1(s)ds + o(ds)$$

$\boldsymbol{M}_1(s+ds)$ is deflected from $\boldsymbol{d}_1(s)$ by the combined rotations of angle τds around $\boldsymbol{d}_3$ and $\kappa_2 ds$ around $\boldsymbol{d}_2$ (fig. 5.5c). Thus, its contribution to the balance of moments onto $\boldsymbol{d}_1(s)$ is :

$$-M_1(s) + M_1(s+ds)\cos(\tau ds)\cos(\kappa_2 ds) = M_1'(s)ds + o(ds)$$

$\boldsymbol{M}_1(s+ds)$ is deflected from $\boldsymbol{d}_1(s)$ by the combined rotations of angle τds around $\boldsymbol{d}_3$ and $\kappa_2 ds$ around $\boldsymbol{d}_2$ (fig. 5.5c). Thus, its contribution to the balance of moments onto $\boldsymbol{d}_2(s)$ is :

$$M_1(s+ds)\sin(\tau ds)\cos(\kappa_2 ds) = \tau M_1(s)ds + o(ds)$$

$\boldsymbol{M}_1(s+ds)$ is deflected from $\boldsymbol{d}_1(s)$ by the combined rotations of angle τds around $\boldsymbol{d}_3$ and $\kappa_2 ds$ around $\boldsymbol{d}_2$ (fig. 5.5c). Thus, its contribution to the balance of moments onto $\boldsymbol{d}_3(s)$ is :

$$-M_1(s+ds)\cos(\tau ds)\sin(\kappa_2 ds) = -\kappa_2 M_1(s)ds + o(ds)$$

$\boldsymbol{Q}(s+ds)$ is deflected from $\boldsymbol{d}_3(s)$ by the combined rotations of angle $\kappa_1 ds$ around $\boldsymbol{d}_1$ and $\kappa_2 ds$ around $\boldsymbol{d}_2$ (fig. 5.5c). Thus, its contribution to the balance of moments onto $\boldsymbol{d}_1(s)$ is :

$$Q(s+ds)\cos(\kappa_1 ds)\sin(\kappa_2 ds) = \kappa_2 Q(s)ds + o(ds)$$

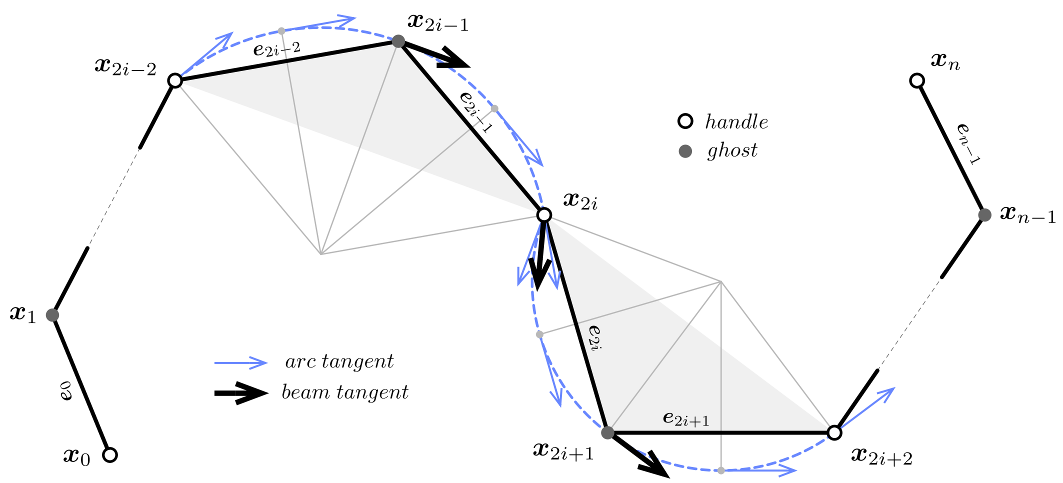

(a) Centerline of the discrete biarc model.

		open	closed
segments	n_s	n_s	n_s
edges	n_e	$2n_s$	$2n_s$
vertices	n	$2n_s + 1$	$2n_s$
ghosts	n_g	n_s	n_s
handles	n_h	$n_s + 1$	n_s

(b) Number of segments, edges and vertices whether the centerline is closed or open.

Figure 5.6 – Biarc model for a discrete beam. The centerline is divided into curved segments (grey solid hatch). Each segment is defined as a three-noded element with uniform material and section properties. It has two end vertices (white) called *handle* as they are used to interact with the model, for instance to apply loads or restrains. It has one mid vertex (grey) called *ghost* as it is used only to enrich the segment kinematics and is not accessible to the end user.

5.7.2 Discret beam model

Let's introduce the discrete biarc model to describe the configuration of a beam. It is composed of a discrete curve called *centerline* and a discrete adapted frame called *material frame* as its axes are chosen to be the principal axes of the beam cross section (fig. 5.6a). The centerline itself is organized in n_s consecutive adjacent segments which are three-vertices and two-edges elements with uniform material and section properties.

Beams can either be closed or open. The corresponding number of vertices, edges and segments are reported in fig. 5.6b.

Centerline

The discrete centerline is a polygonal space curve (fig. 5.6a) defined as an ordered sequence of $n+1$ pairwise disjoint *vertices* : $\Gamma = (\boldsymbol{x}_0, \boldsymbol{x}_1, \dots, \boldsymbol{x}_n) \in \mathbb{R}^{3(n+1)}$. Consecutive pairs of vertices define n straight segments $(\boldsymbol{e}_0, \boldsymbol{e}_1, \dots, \boldsymbol{e}_{n-1})$ called *edges* and pointing from one vertex to the next one : $\boldsymbol{e}_i = \boldsymbol{x}_{i+1} - \boldsymbol{x}_i$:

$$\begin{cases} \boldsymbol{e}_i = \boldsymbol{x}_{i+1} - \boldsymbol{x}_i \\ l_i = \|\boldsymbol{e}_i\| \\ \boldsymbol{u}_i = \boldsymbol{e}_i / l_i \end{cases} \tag{5.47}$$

The length of the ith edge is denoted l_i and its normalized direction vector is denoted $\boldsymbol{u}_i$. The arc length of the ith vertex is denoted s_i and is given by :

$$\begin{cases} s_0 = 0 & i = 0 \\ s_i = \sum_{k=0}^{i-1} l_k & i \in [\![1, n-1]\!] \\ s_n = L & i = n \end{cases} \tag{5.48}$$

Thus, the centerline is parametrized by arc length and $\Gamma(s_i) = \boldsymbol{x}_i$. Additionally, we define the vertex-based mean length at vertex $\boldsymbol{x}_i$:

$$\begin{cases} \overline{l_0} = \frac{1}{2} l_0 & i = 0 \\ \overline{l_i} = \frac{1}{2}(l_{i-1} + l_i) & i \in [\![1, n-1]\!] \\ \overline{l_n} = \frac{1}{2} l_{n-1} & i = n \end{cases} \tag{5.49}$$

Segments

The discrete centerline is divided into n_s curved segments. Each segment is a three-noded element – see fig. 5.6a where the area covered by a segment is represented as a grey solid hatch. The ith segment is composed of three vertices $(\boldsymbol{x}_{2i}, \boldsymbol{x}_{2i+1}, \boldsymbol{x}_{2i+2})$ spanning two edges $(\boldsymbol{e}_{2i}, \boldsymbol{e}_{2i+1})$. The (i-1)th segment and the ith segment share the same vertex $\boldsymbol{x}_{2i}$ at arc length s_{2i}.

Each segment has two end vertices called *handle* ($\boldsymbol{x}_{2i}, \boldsymbol{x}_{2i+2}$) and one mid vertex called *ghost* ($\boldsymbol{x}_{2i+1}$) as this one is not accessible to the end user in order to interact with the model (link, restrain, loading, ...). Ghost vertices are used only for internal purpose to give a higher richness in the kinematic description of a segment than a two-noded segment would.

We define the *chord length* of the ith segment as the distance between $\boldsymbol{x}_{2i}$ and $\boldsymbol{x}_{2i+2}$: $L_i = \|\boldsymbol{e}_{2i} + \boldsymbol{e}_{2i+1}\|$.

Material and section properties

In addition, the model assumes that a segment has uniform section (S, I_1, I_2, J)[24] and material (E, G)[25] properties over its length : $s \in]s_{2i}, s_{2i+2}[$. For the sake of simplicity, we introduce for further calculations the *material stiffness matrix* ($\boldsymbol{B}_i$) attached to each segment. It has the following form in the material frame basis :

$$\boldsymbol{B}_i = \begin{bmatrix} EI_1 & 0 & 0 \\ 0 & EI_2 & 0 \\ 0 & 0 & GJ \end{bmatrix}_i \tag{5.50}$$

External loads

Also, the model assumes that each segment can be loaded with uniform external distributed forces ($\boldsymbol{f}_{ext}$) and moments ($\boldsymbol{m}_{ext}$).

External loads

External concentrated forces ($\boldsymbol{F}_{ext}$) and moments ($\boldsymbol{M}_{ext}$) are applied to the segment end vertices ($\boldsymbol{x}_{2i}$, $\boldsymbol{x}_{2i+2}$).

This discret model involves that axial, bending and torsion strains, section and material properties will be continuous fonctions of the arc length over each segment $]\boldsymbol{x}_{2i}, \boldsymbol{x}_{2i+2}[$. Discontinuities in strains, internal and external forces, internal and external moments will be located at handle vertices. The left and right limits of this fonctions at handle vertices will be denoted respectively by f^- and f^+. Possibly they are continuous at handle nodes that is the left and right limits agree ($f^- = f^+$).

Lets call : $l_i = \|\boldsymbol{e}_i\|$ with $i \in [0, n_e]$. Lets call : $u_i = \frac{e_i}{l_i}$ with $i \in [0, n_e]$.

Lets call : $L_i = \|\boldsymbol{e}_{2i} + \boldsymbol{e}_{2i+1}\|$ with $i \in [0, n_g]$.

We have : $\boldsymbol{d}_{3,i+1/2} = \boldsymbol{u}_i$

Let $\boldsymbol{B}_i$ be the material stiffness matrix along the principal axes of inertia, uniform over

[24] S is the cross section area ; I_1, I_2 and J are the cross section principal moments of inertia.
[25] E is the elastic modulus and G is the shear modulus for the considered material

the slice $]\boldsymbol{x}_{2i}, \boldsymbol{x}_{2i+2}[$. Thus, it has the following form in the material basis :

$$\boldsymbol{B}_i = \begin{bmatrix} EI_1 & 0 & 0 \\ 0 & EI_2 & 0 \\ 0 & 0 & GJ \end{bmatrix}_i \tag{5.51}$$

Thus, one will write the constitutive equations for the bending moment in matrix notation as :

$$\boldsymbol{M}_i = \boldsymbol{B}_i(\boldsymbol{\kappa b}_i - \overline{\boldsymbol{\kappa b}}_i) \tag{5.52}$$

With $\boldsymbol{\kappa b} = \begin{bmatrix} \kappa_1 & \kappa_2 & \tau \end{bmatrix}^T$ expressed in the material frame.

5.7.3 Discret bending moments and curvatures

We assume that the internal bending moment and curvature are quadratic functions of the arc length over $]\boldsymbol{x}_{2i}, \boldsymbol{x}_{2i+2}[$. While they must be continuous over this interval, they might be discontinuous at handle vertices and be subjected to jump discontinuities in direction and magnitude.

Curvature at ghost vertices

For a given geometry of the centerline, the curvature binormal vector at ghost vertex $\boldsymbol{x}_{2i-1}$ (resp. $\boldsymbol{x}_{2i+1}$) is computed considering the circumscribed osculating circle passing through the vertices $(\boldsymbol{x}_{2i-2}, \boldsymbol{x}_{2i-1}, \boldsymbol{x}_{2i})$ of the $(i-1)th$ segment – resp. through the vertices $(\boldsymbol{x}_{2i}, \boldsymbol{x}_{2i+1}, \boldsymbol{x}_{2i+2})$ of the i-th segment.

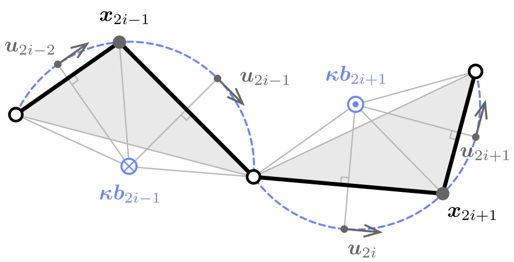

$$\kappa\boldsymbol{b}_{2i-1} = \frac{2}{L_{i-1}}\boldsymbol{u}_{2i-2} \times \boldsymbol{u}_{2i-1}$$

$$\kappa\boldsymbol{b}_{2i+1} = \frac{2}{L_i}\boldsymbol{u}_{2i} \times \boldsymbol{u}_{2i+1}$$

Unit tangent vectors at ghost vertices

This definition of the curvature leads to a natural definition of the unit tangent vector at ghost vertex $\boldsymbol{x}_{2i-1}$ (resp. $\boldsymbol{x}_{2i+1}$), as the unit vector tangent to the osculating circle of the $(i-1)th$ segment (resp. i-th segment) at that point.

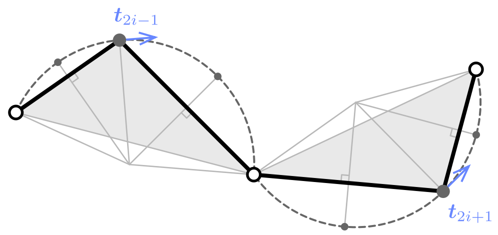

$$\boldsymbol{t}_{2i-1} = \frac{l_{2i-1}}{L_{i-1}}\boldsymbol{u}_{2i-2} + \frac{l_{2i-2}}{L_{i-1}}\boldsymbol{u}_{2i-1}$$

$$\boldsymbol{t}_{2i+1} = \frac{l_{2i+1}}{L_i}\boldsymbol{u}_{2i} + \frac{l_{2i}}{L_i}\boldsymbol{u}_{2i+1}$$

Left/right unit tangent vectors at handle vertices

Equivalently, the definition of the osculating circles of the $(i-1)th$ and i-th segments leads to a natural definition of the left ($\boldsymbol{t}_{2i}^-$) and right ($\boldsymbol{t}_{2i}^+$) unit tangent vectors at handle vertex $\boldsymbol{x}_{2i}$, for segments of uniform curvature. When both segments have the same curvature, left and right vectors agree.

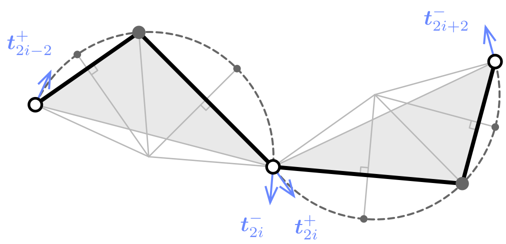

$$\boldsymbol{t}_{2i}^- = 2(\boldsymbol{t}_{2i-1} \cdot \boldsymbol{u}_{2i-1})\boldsymbol{u}_{2i-1} - \boldsymbol{t}_{2i-1}$$

$$\boldsymbol{t}_{2i}^+ = 2(\boldsymbol{t}_{2i+1} \cdot \boldsymbol{u}_{2i})\boldsymbol{u}_{2i} - \boldsymbol{t}_{2i+1}$$

Unit tangent vectors at handle vertices

The unit tangent vector $\boldsymbol{t}_{2i}$ – that is the beam section normal – at handle vertex $\boldsymbol{x}_{2i}$ is chosen to be the mean of the left and right unit tangent vectors at that vertex.[26]

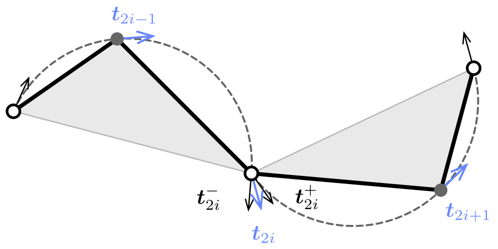

$$\boldsymbol{t}_{2i} = \frac{\boldsymbol{t}_{2i}^- + \boldsymbol{t}_{2i}^+}{\|\boldsymbol{t}_{2i}^- + \boldsymbol{t}_{2i}^+\|}$$

This way, the determination of the tangent vectors – or equivalently the section normals – in the static equilibrium configuration will be done in the flow of the dynamic relaxation process, without the need of introducing any additional degrees of freedom (for instance the usual Euler angles). The position of the vertices rules the orientation of the section normals.

Left/right bending moments at handle vertices

Given the unit tangent vector $\boldsymbol{t}_{2i}$, one can define the left ($\boldsymbol{\kappa}_{2i}^-$) and right ($\boldsymbol{\kappa}_{2i}^+$) curvatures at handle vertex $\boldsymbol{x}_{2i}$. The left curvature is initially evaluated from the left osculating circle, defined as the circle passing through $\boldsymbol{x}_{2i-1}$ and $\boldsymbol{x}_{2i}$ and tangent to $\boldsymbol{t}_{2i}$ at $\boldsymbol{x}_{2i}$. The right curvature is initially evaluated from the right osculating circle, defined as the circle passing through $\boldsymbol{x}_{2i}$ and $\boldsymbol{x}_{2i+1}$ and tangent to $\boldsymbol{t}_{2i}$ at $\boldsymbol{x}_{2i}$.[27,28]

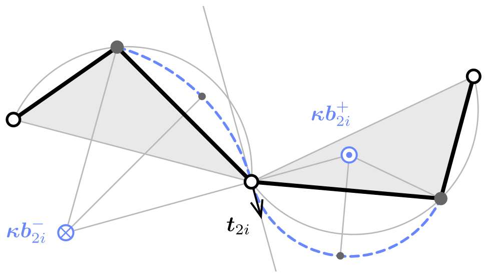

$$\boldsymbol{\kappa b}_{2i}^- = \frac{2}{l_{2i-1}} \boldsymbol{u}_{2i-1} \times \boldsymbol{t}_{2i}$$
$$\boldsymbol{\kappa b}_{2i}^+ = \frac{2}{l_{2i}} \boldsymbol{t}_{2i} \times \boldsymbol{u}_{2i}$$

However, this values need to be adjusted so that the static condition for rotational equilibrium ($\boldsymbol{M}^{ext} + \boldsymbol{M}^+ - \boldsymbol{M}^- = 0$) is satisfied at all time. Then, this condition will be satisfied – in particular – at the end of the solving process. To achieve this goal, we first

[26] Consequently, this model assumes that the field of tangents along the centerline is continuous and is thus unable to model cases where the centerline is not at least $\mathcal{C}^1$. In such case the beam must be considered as two parts glued together.

[27] Remark that the centerline is now approximated with a biarc in the vicinity of $\boldsymbol{x}_{2i}$. This is the reason why this model is called the "biarc model".

[28] This model offers the ability to represent discontinuities in curvature – thus in bending moment – at handle vertices as the left and right curvatures does not necessarily agree. This is quite different from the classical 3-dof element [Bar99, ABW99, DBC06] which assumes that the curvature – thus the bending moment – is $\mathcal{C}^0$ and can be evaluated at every vertices from the circumscribed osculating circle.

compute a realistic mean value ($\boldsymbol{M}_{2i}$) for the internal bending moment as :

$$\boldsymbol{M}_{2i} = \frac{1}{2}\boldsymbol{B}_{i-1}(\boldsymbol{\kappa b}^{-}_{2i} - \overline{\boldsymbol{\kappa b}}^{-}_{2i}) + \frac{1}{2}\boldsymbol{B}_{i}(\boldsymbol{\kappa b}^{+}_{2i} - \overline{\boldsymbol{\kappa b}}^{+}_{2i}) \tag{5.53}$$

To enforce the jump discontinuity in bending moment ($\boldsymbol{M}^{ext} = \boldsymbol{M}^{-} - \boldsymbol{M}^{+}$) across the handle vertex, we define the left and right bending moments at $\boldsymbol{x}_{2i}$ as :

$$\boldsymbol{M}^{-}_{2i} = \boldsymbol{M}_{2i} + \frac{1}{2}\boldsymbol{M}^{ext}_{2i} \tag{5.54a}$$

$$\boldsymbol{M}^{+}_{2i} = \boldsymbol{M}_{2i} - \frac{1}{2}\boldsymbol{M}^{ext}_{2i} \tag{5.54b}$$

Note that in the case where no external concentrated bending moment is applied to the handle vertex, the internal bending moment is continuous across the vertex.

Left/right curvatures at handle vertices

Finally, the left and right curvatures at handle vertex $\boldsymbol{x}_{2i}$ are computed back with the constitutive law :

$$\boldsymbol{\kappa b}^{-}_{2i} = \boldsymbol{B}^{-1}_{i-1}\boldsymbol{M}^{-}_{2i} + \overline{\boldsymbol{\kappa b}}^{-}_{2i} \tag{5.55a}$$

$$\boldsymbol{\kappa b}^{+}_{2i} = \boldsymbol{B}^{-1}_{i}\boldsymbol{M}^{+}_{2i} + \overline{\boldsymbol{\kappa b}}^{+}_{2i} \tag{5.55b}$$

Bending moment at ghost vertices

The internal bending moment at ghost vertices is simply given by the constitutive law as :

$$\boldsymbol{M}_{2i-1} = \boldsymbol{B}_{i-1}(\boldsymbol{\kappa b}_{2i-1} - \overline{\boldsymbol{\kappa b}}_{2i-1}) \tag{5.56a}$$

$$\boldsymbol{M}_{2i+1} = \boldsymbol{B}_{i}(\boldsymbol{\kappa b}_{2i+1} - \overline{\boldsymbol{\kappa b}}_{2i+1}) \tag{5.56b}$$

5.7.4 Discret twisting moment

We assume the twisting moment and the rate of twist to vary linearly over $]\boldsymbol{x}_{2i}, \boldsymbol{x}_{2i+2}[$. Thus, the rate of twist at mid edge is given by :

$$\tau_{i+1/2} = \frac{\Delta\theta_i}{l_i} \tag{5.57}$$

And $\theta_{i+1} - \theta_i$ is the additional twisting angle between two frames with parallel transport.

$$Q_{i+1/2} = GJ(\tau_{i+1/2} - \overline{\tau}_{i+1/2}) \tag{5.58}$$

5.7.5 Discret axial force

We assume the axial force and the axial strain to vary linearly over $]\boldsymbol{x}_{2i}, \boldsymbol{x}_{2i+2}[$. Thus, the axial strain at mid edge is given by :

$$\epsilon_{i+1/2} = \frac{l_i}{\bar{l}_i} - 1 \tag{5.59}$$

$$N_{i+1/2} = ES\epsilon_{i+1/2} \tag{5.60}$$

5.7.6 Discret shear force

Shear forces are computed from the second Kirchhoff law, considering that the inertial term is negligible.

$$\boldsymbol{F}_{i+1/2} = \boldsymbol{d}_{3,i+1/2} \times (\boldsymbol{M}'_{i+1/2} + \boldsymbol{m}_{ext,i}) + Q_{i+1/2}\boldsymbol{\kappa b}_{i+1/2} - \tau_{i+1/2}\boldsymbol{M}_{i+1/2} \tag{5.61}$$

5.7.7 Interpolation

5.8 Conclusion

Remind that the beam is subject to a distributed external force $\boldsymbol{f}_{ext}$ and a distributed external moment $\boldsymbol{m}_{ext}$.

We neglect rotational inertial effects on $\boldsymbol{d}_1$ et $\boldsymbol{d}_2$ in (**??**) and (**??**) which leads to the following shear force :

$$\boldsymbol{F}^{\perp}(s) = \boldsymbol{d}_3 \times (\boldsymbol{M}' + \boldsymbol{\Omega} \times \boldsymbol{M} + \boldsymbol{m}_{ext}) \tag{5.62}$$

$$\boldsymbol{F}^{\parallel}(s) = N\boldsymbol{d}_3 \tag{5.63}$$

We may neglect as well the last term ($\tau\boldsymbol{M}$) and get back to the shear force obtained by the variational approach.The total internal force acting on the beam is hence given by :

$$\boldsymbol{F}(s) = \boldsymbol{N}(s) + \boldsymbol{T}(s) \tag{5.64}$$

Sections are subject to the following rotational moment around the centerline :

$$\boldsymbol{\Gamma}(s) = Q' + \boldsymbol{d}_3 \cdot (\kappa\boldsymbol{b} \times \boldsymbol{M} + \boldsymbol{m}_{ext}) \tag{5.65}$$

Bibliography

[AAP10] Basile Audoly, M Amar, and Yves Pomeau. *Elasticity and geometry.* 2010.

[ABW99] Sigrid Adriaenssens, Michael Barnes, and Christopher Williams. A new analytic and numerical basis for the form-finding and analysis of spline and gridshell structures. In B Kumar and B H V Topping, editors, *Computing Developments in Civil and Structural Engineering*, pages 83–91. Civil-Comp Press, Edinburgh, 1999.

[Ant74] Stuart Antman. Kirchhoff's problem for nonlinearly elastic rods. *Quarterly of Applied Mathematics*, XXXIV(3):221–240, 1974.

[Ant05] Stuart Antman. *Nonlinear problems of elasticity.* Applied mathematical sciences. Springer, New York, 2005.

[BAK13] Michael Barnes, Sigrid Adriaenssens, and Meghan Krupka. A novel torsion/bending element for dynamic relaxation modeling. *Computers & Structures*, 119:60–67, apr 2013.

[Bar99] Michael Barnes. Form finding and analysis of tension structures by dynamic relaxation. *International Journal of Space Structures*, 14(2):89–104, 1999.

[BAV+10] Miklós Bergou, Basile Audoly, Etienne Vouga, Max Wardetzky, and Eitan Grinspun. Discrete viscous threads. *ACM Transactions on ...*, pages 1–10, 2010.

[Ben91] Edoardo Benvenuto. *An introduction to the history of structural mechanics : vaulted structures and elastic systems.* Springer Verlag, New York, 1991.

[CBd13] Romain Casati and Florence Bertails-descoubes. Super space clothoids. In *SIGGRAPH*, 2013.

[CDL+93] Bernard Coleman, Ellis Harold Dill, Mazario Lembo, Lu Zheng, and Irwin Tobias. On the Dynamics of Rods in the Theory of Kirchhoff and Clebsch. *Archive for Rational Mechanics and Analysis*, 121(4):339–359, 1993.

[CH02] J Cisternas and P Holmes. Buckling of extensible thermoelastic rods. *Mathematical and Computer Modelling*, 36(3):233–243, 2002.

[Cle83] Alfred Clebsch. *Théorie de l'élasticité des corps solides.* Dunod, Paris, 1883.

[DA14] Marcelo A. Dias and Basile Audoly. A non-linear rod model for folded elastic strips. *Journal of the Mechanics and Physics of Solids*, 62(1):57–80, 2014.

[DA15] Marcelo A. Dias and Basile Audoly. "Wunderlich, meet kirchhoff" : a general and unified description of elastic ribbons and thin rods. *Journal of Elasticity*, 119(1):49–66, 2015.

[Day65] Alister Day. An Introduction to dynamic relaxation. *The Engineer*, 1965.

[DBC06] Cyril Douthe, Olivier Baverel, and Jean-François Caron. Formfinding of a grid shell in composite materials. *Journal of the IASS*, 47:53–62, 2006.

[Dil92] Ellis Harold Dill. Kirchhoff's theory of rods. *Archive for History of Exact Sciences*, page 23, 1992.

[DKZ14] B. D'Amico, A. Kermani, and H. Zhang. Form finding and structural analysis of actively bent timber grid shells. *Engineering Structures*, 81:195–207, 2014.

[DLP13] Ye Duan, Dong Li, and P. Frank Pai. Geometrically exact physics-based modeling and computer animation of highly flexible 1D mechanical systems. *Graphical Models*, 75(2):56–68, 2013.

[dPTL+15] Lionel du Peloux, Frédéric Tayeb, Baptiste Lefevre, Olivier Baverel, and Jean-François Caron. Formulation of a 4-DoF torsion / bending element for the formfinding of elastic gridshells. In *Proceedings of the International Association for Shell and Spatial Structures*, number August, pages 1–14, Amsterdam, 2015.

[DZK16] B. D'Amico, H. Zhang, and A. Kermani. A finite-difference formulation of elastic rod for the design of actively bent structures. *Engineering Structures*, 117:518–527, 2016.

[Hoo06] P C J Hoogenboom. 7 Vlasov torsion theory. (October):1–12, 2006.

[Kir50] Gustav Kirchhoff. *Über das gleichgewicht und die bewegung einer elastischen scheibe*. Berlin, 1850.

[Kir76] Gustav Kirchhoff. *Vorlesungen über mathematische, physik, mechanik*. Leipzig, 1876.

[LL09] Holger Lang and Joachim Linn. Lagrangian field theory in space-time for geometrically exact Cosserat rods. 150:21, 2009.

[Lov92] Augustus Love. *A treatise on the mathematical theory of elasticity*. Cambridge University Press, first edition, 1892.

[LS96] Joel Langer and David Singer. Lagrangian Aspects of the Kirchhoff elastic rod. *Society for Industrial and Applied Mathematics Review*, 38(4):605–618, 1996.

[MLG13] D.E. Moulton, Th. Lessinnes, and A Goriely. Morphoelastic rods. Part I : A single growing elastic rod. *Journal of the Mechanics and Physics of Solids*, 61(2):398–427, 2013.

[MPW14] Christoph Meier, Alexander Popp, and Wolfgang A. Wall. An objective 3D large deformation finite element formulation for geometrically exact curved Kirchhoff rods. *Computer Methods in Applied Mechanics and Engineering*, 278(August):445–478, 2014.

[Neu09] S. Neukirch. *Enroulement, contact et vibrations de tiges élastiques*. PhD thesis, 2009.

[SBH95] Yaoming Shi, Andrey E. Borovik, and John E. Hearst. Elastic rod model incorporating shear and extension, generalized nonlinear Schrödinger equations, and novel closed-form solutions for supercoiled DNA. *The Journal of Chemical Physics*, 103(8):3166–3183, 1995.

[Spi08] Jonas Spillmann. *CORDE : Cosserat rod elements for the animation of interacting elastic rods.* PhD thesis, 2008.

[TG51] Stephen Timoshenko and James Norman Goodier. *Theory of elasticity.* McGraw-Hill, New York, second edition, 1951.

[The07] Adrien Theetten. *Splines dynamiques géométriquement exactes : simulation haute performance et interaction.* PhD thesis, Université des Sciences et Technologies de Lille, 2007.

[Tim21] Stephen Timoshenko. On the correction for shear of the differential equation for transverse vibrations of prismatic bars. *Philosophical Magazine Series 6*, 41(245):744–746, 1921.

[Tim22] Stephen Timoshenko. On the transverse vibrations of bars of uniform cross-section. *Philosophical Magazine Series 6*, 43(253):125–131, 1922.

[Vet14] Yury Vetyukov. *Nonlinear mechanics of thin-walled structures : asymptotics, direct approach and numerical analysis.* 1 edition, 2014.

[Vil97] Piero Villaggio. *Mathematical models for elastic structures.* Cambridge University Press, 1997.

[Wak80] David Wakefield. *Dynamic relaxation analysis of pretensioned networks supported by compression arches.* PhD thesis, City University London, 1980.